Pakistan Veterinary Journal

ISSN: 0253-8318 (PRINT), 2074-7764 (ONLINE)
DOI: 10.29261/pakvetj/2023.077

RESEARCH ARTICLE

Platelet-Rich Plasma in Vitrification; is it Helpful or Harmful?

Türker Çavuşoğlu[1*], Aylin Gökhan[2], Canberk Tomruk[3], Cansın Şirin[2], Kubilay Doğan Kılıç[2] and Gürkan Yiğittürk[4]

[1]Department of Histology and Embryology, Faculty of Medicine, Izmir Bakircay University, Izmir, Turkiye
[2]Department of Histology and Embryology, Faculty of Medicine, Ege University, Izmir, Turkiye
[3]Department of Histology and Embryology, Republic of Turkey Ministry of Health Samsun Education and Research Hospital, Samsun, Turkiye
[4]Department of Histology and Embryology, Faculty of Medicine, Mugla Sitki Kocman University, Izmir, Turkiye
*Corresponding author: turker.cavusoglu@bakircay.edu.tr

ARTICLE HISTORY (23-098)

Received:	March 25, 2023
Revised:	June 19, 2023
Accepted:	June 23, 2023
Published online:	September 05, 2023

Key words:
Platelet-Rich Plasma
Vitrification
Cryopreservation
Ethylene Glycol
Dimethyl Sulfoxide
Calcium

ABSTRACT

Human and animal studies on cryoprotectants and freezing solutions are still needed to establish a simple yet reliable protocol and increase the success of cryopreservation. The main aim of this study was to evaluate the short- and long-term effects of platelet-rich plasma, a well-known antioxidant substance due to its contents including bioactive molecules and growth factors, on whole ovarian tissue cryopreservation. Fresh tissues (control group, G1) were subjected to histological tissue processing without any treatment. Ovaries treated with platelet-rich plasma (PRP)-supplemented vitrification solution were subjected to tissue processing without cryostorage group 2 (G2) or following six months of cryostorage group 3 (G3). Steps in G2 and G3 were also performed for group 4 (G4) and group 5 (G5), respectively, except that the vitrification solution was supplemented with fetal bovine serum. PRP was activated with calcium chloride ($CaCl_2$) after double centrifugation. Ethylene glycol, dimethyl sulfoxide, and sucrose were used as cryoprotective agents in all groups. Histomorphological changes were evaluated with the semi-quantitative histochemical-scoring algorithm. Apoptotic and antiapoptotic effects and intercellular connections were evaluated with immunohistochemical staining of Bax, Bcl-2, Caspase-3 (C3), Connexin-43 (Cx-43), and TUNEL analysis. Cryopreservation with PRP-supplementation (G3) significantly increased tissue degeneration ($p<0.05$). There was an increase in the number of degenerated both primary and secondary follicles ($p<0.05$), and an increase in the immune expression of Bax, C3 and Cx-43 and TUNEL assay in G3 was observed compared to other groups ($p<0.05$). Since the morphology of primordial follicles was more preserved than other follicles in all groups, primordial follicles were not included in the follicle count. Our study suggested that cryopreservation with PRP-supplemented vitrification solution caused excessive damage to rat ovaries. We assumed that $CaCl_2$ might have further provoked this cellular damage.

To Cite This Article: Çavuşoğlu T, Gökhan A, Tomruk C, Şirin C, Kılıç KD, Yiğittürk G, 2023. Platelet-rich plasma in vitrification; is it helpful or harmful?. Pak Vet J, 43(3): 500-506. http://dx.doi.org/10.29261/pakvetj/2023.077

INTRODUCTION

Ovarian tissue cryopreservation (OTCP), which was mentioned as an experimental model in the previous board decision but was declared non-experimental in the latest current opinion, offers an excellent option to preserve the highest number of follicles that increases the probability of fertilization (Practice Committee of the American Society for Reproductive Medicine, 2019). Since it is known that OTCP frequently disrupts the DNA integrity, function, and structure of ovarian tissue and cryoprotective agents (CPAs) are also toxic, this study aims to develop OTCP methods by optimizing the content of the vitrification solution.

Vitrification is the freezing of cells or tissues in a glassy structure at rapid cooling rates without ice crystallization using vitrification solutions containing CPAs (Schallmoser *et al.*, 2022). Ethylene glycol (EG) and dimethyl sulfoxide (DMSO) are among the most preferred CPAs being used in OTCP, but CPAs are toxic and there is a need for animal studies based on supplementing CPA blends with serum components or antioxidant agents

(Oktay, 2022). Studies adding human or animal serum components such as Human Serum Albumin or Fetal Bovine Serum (FBS) to the vitrification solution are available in the literature, but concerns about FBS containing exogenous non-human material, xenoproteins, and contaminants lead researchers to reduce the use of FBS or seek an alternative antioxidant supplement.

At this point, serum components obtained from human blood, in particular platelet-rich plasma (PRP), emerges as the most promising alternative substitute. Characterized as a cellular plasma component, PRP plays an antioxidant role in vascular reactivity and angiogenesis, healing, and tissue repair due to the growth factors, cytokines, and bioactive molecules it contains. It promises a glorious future in reproductive medicine with its therapeutic use such as menstruation recovery and pregnancy by intraovarian injection (Merhi *et al.*, 2022). However, the number of studies using PRP as a preservative in cryopreservation protocols is very limited.

Cryopreservation of whole rat ovarian tissue with the addition of PRP to the vitrification solution will allow the evaluation of the effects of PRP on short- and long-term cryopreservation. The results of this study are expected to offer an innovative approach to cryopreservation protocols and contribute to infertility treatment and ovarian tissue biobanking research.

MATERIALS AND METHODS

Animals and ethics approval: Thirty-five female Wistar rats, 8-12 weeks old, housed in standard conditions were exposed to 12 hours of light/dark cycles at room temperature and fed *ad libitum*. At the end of the experiment, the animals were anesthetized with ketamine hydrochloride (Pfizer) xylazine (Bayer) (80/10 mg/kg, IP) combination and sacrificed. Animals were provided by the Ege University Laboratory Animals Application and Research Center with the approval of the Local Ethics Committee (date 26.12.2018, #2018-131).

Experimental design: The scheme of the experimental design is given in Fig. 1. Rats were randomly divided into five groups (G1-5) (n=7 per group). G1 was the fresh control group (non-vitrified) with no application. In two of the study groups (Groups 2 and 3), a vitrification solution containing autologous PRP was used, while in the other two study groups (Groups 4 and 5), a vitrification solution containing animal-derived FBS was used for comparison. Two of the study groups (Groups 3 and 5) were stored in liquid nitrogen at -196°C for 6 months to comparatively examine the long-term effect of vitrification with PRP-containing solution. Finally, all groups, including the control group, were examined microscopically by histochemical and immunohistochemical staining.

PRP preparation: The method of PRP preparation was modified from (Chen *et al.*, 2018). The harvested blood was anticoagulated with 3.2% sodium citrate at the ratio of 9:1 blood/citrate and centrifuged at 200G (20 min, 4°C). The supernatant with a buffy coat was pipetted into empty tubes and centrifuged at 480G (10 min, 4°C). The supernatant (platelet-poor plasma) was removed. The bottom layer (PRP) was activated with 10% (w/v) calcium chloride ($CaCl_2.6H_2O$) solution to obtain a concentration of approximately 0.46 M $CaCl_2$. The final $CaCl_2$-activated PRP was used as the content of the vitrification solution.

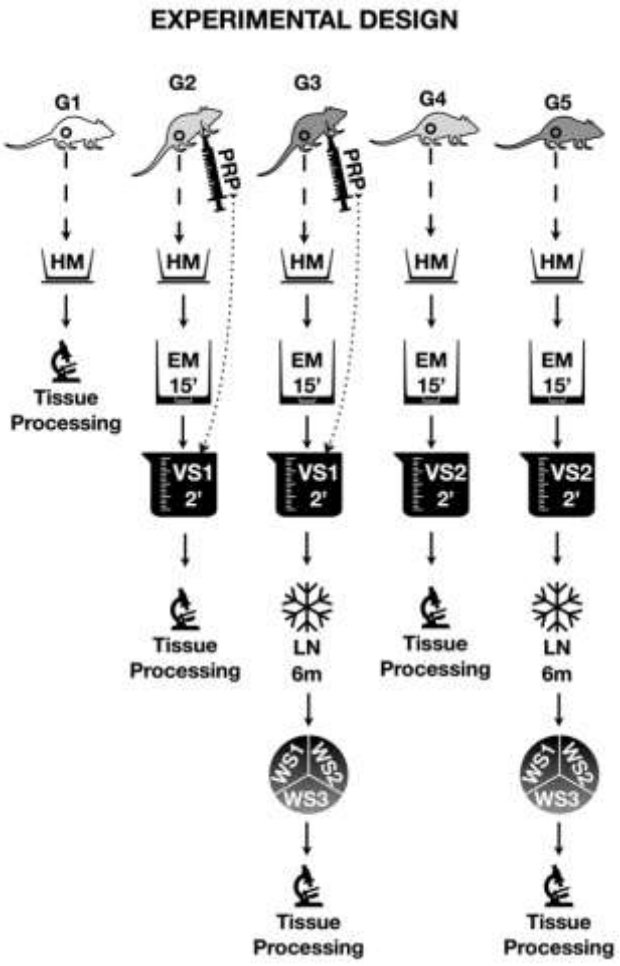

Fig. 1: The scheme of the experimental design. *HM: Handling Medium; EM: Equilibration Medium; VS: Vitrification Solution; WS: Warming Solution. LN: Liquid Nitrogen.*

Preparation of solutions and cryopreservation: The freezing/thawing method was modified from the study of (He *et al.*, 2018). The ovaries transported to the laboratory in the handling medium (HM) were then transferred to the equilibration medium (EM) and held for 15 minutes. Then, G2 and G3 ovaries were transferred to the PRP-supported vitrification solution (VS1), while G4 and G5 ovaries were transferred to the FBS-supported one (VS2). All groups were kept in respective vitrification solutions for 2 minutes. The components of the solutions are itemized in Table 1.

Microscopic examination of ovaries

Tissue processing and stainings: All ovaries were fixed in 4% paraformaldehyde. After routine tissue processing procedure and paraffin embedding, paraffin blocks were sectioned at five µm and stained. All stained sections were examined under the camera (Olympus DP72, Tokyo, Japan) attached to the microscope (Olympus BX51, Tokyo, Japan) with the analysis tools (Olympus CellSens Software and Fiji by ImageJ).

Table 1: Content of cryopreservation solutions.

	HM	EM	VITRIFICATION		WARMING		
			VS1	VS2	WS1	WS2	WS3
DMEM/F-12 (Sigma)	90%	80%	50%	50%	100%	100%	100%
FBS (Gibco)	10%			10%			
PRP			10%				
EG (Sigma)		10%	20%	20%			
DMSO (Sigma)		10%	20%	20%			
S (Merck)			0.5 mol/L	0.5 mol/L	0.5 mol/L	0.25 mol/L	0.125 mol/L

HM: Handling Medium; EM: Equilibration Medium; VS: Vitrification Solution; WS: Warming Solution; DMEM/F-12: Dulbecco's Modified Eagle Medium/Nutrient Mixture F-12; FBS: Fetal Bovine Serum; PRP: Platelet-Rich Plasma; EG: Ethylene Glycol; DMSO: Dimethyl Sulfoxide; S: Sucrose.

Table 2: Criteria and scoring algorithm for microscopic evaluation of HC-stainings.

A. Criteria of semi-quantitative analysis
Parenchyma (follicular components)
Follicles
Corpus luteum
Stroma (non-follicular components)
Ovarian surface epithelium
Tunica albuginea
Blood vessels, nerves, lymphatic vessels
Stromal cells (fibrocytes and interstitial cells)
Connective tissue components (collagen and reticular fibers)

B. Algorithm for HC-scoring of criteria		
Grade	Severity	Proportion
0	Unremarkable	Negligible
1	Minimal	Rare
2	Mild	Few
3	Distinct	Moderate
4	Strong	Common
5	Severe	Diffuse

HC examination and follicle counting: Sections were stained with Hematoxylin and Eosin (HE), Periodic Acid Schiff (PAS), and Masson Trichrome (MT) to reveal the histomorphological changes. HE staining was performed according to the routine protocol. PAS (Bio-optica) and MT (Bio-optica) stainings were performed with the manufacturer's kits according to the instructions. Histomorphological changes in both parenchyma and stroma of the ovary were examined following the literature (Kinnear *et al.*, 2020) and the semi-quantitative analyses were scored with the HC-scoring algorithm (Table 2). One slide per animal for each HC scoring was randomly selected. Three blinded histologists independently performed a semi-quantitative analysis on the whole slide at different magnifications according to the criteria given in Table 2 (A) and graded these criteria using the HC-scoring algorithm given in Table 2 (B). The final HC-score was obtained by the mean of three observers. The evaluation of ovarian follicles was based on previous literature (Gandolfi *et al.*, 2006). Healthy and degenerated primary and secondary follicles were defined by considering the histomorphological criteria such as pycnosis, eosinophilic cytoplasm, the integrity of zona pellucida and granulosa cells, and follicles were counted by three blind histologists for statistical analysis. Primordial follicles were not taken into consideration since their morphology was mostly preserved in each group.

IHC assessment and TUNEL assay: The activation of apoptotic-antiapoptotic pathways and cellular connections were assessed with IHC staining of Bax (1:100 dilution, BS-0127R, Bioss-USA), Bcl-2 (1:100 dilution, Sc-7382, Santa Cruz, USA), Caspase-3 (C3) (1:100 dilution, A0835-1, Acris), and Connexin-43 (Cx-43) (1:100 dilution, Bs-0651R, Bioss-USA). TdT-mediated dUTP Nick-End Labeling (TUNEL) assay (Roche) was performed to detect cellular damage, especially follicular degeneration, and to determine the protective effect of PRP. TUNEL assay was performed with the staining kit following the manufacturer's instructions. The immunohistochemical labeling was evaluated semi-quantitatively by three histologists in a blinded fashion. The percentage of the positive immunostained area was calculated over six randomly selected fields at 400x magnification and the mean of three observers was recorded as the final IHC score.

Statistical analysis: Statistical analysis was performed with IBM SPSS Statistics for Windows, Version 25.0. Normal distribution was analyzed with the Shapiro-Wilk Test on one-way analysis of variance. Of the variables, the number of follicles matched the normal distribution, while the positive immunostained area did not. Normal distributions were evaluated with a One-Way Analysis of Variance between groups, checked with Levene's Test, and F statistic was used for multiple group comparisons, and the Tukey HSD method was used as post-HOC for pairwise comparisons. Kruskal Wallis and post hoc Dunn's Test (Bonferroni corrected) were used in those that did not fit the normal distribution. All hypothesis tests were performed at 0.05 Type I error level.

RESULTS

Results of HC examination: Sections of G1 showed regular histomorphology (Fig. 2-a, f, k). Severe histomorphological damage with marked degeneration of primary and secondary follicles is particularly observed in G2 (Fig. 2-b, g, l) and G3 (Fig. 2-c, h, m). Tissue damage in G2 (Fig. 2-b, g, I) is less pronounced than tissue damage in G3 (Fig. 2-c, h, m) and more pronounced than tissue damage in G5 (Fig. 2-e, j, o). G4 (Fig. 2-d, i, n) showed the least damage among all experimental groups. Representative sections of HC stainings are presented in Fig. 2.

Results of HC-scoring and follicle counting: The degeneration severity of tissue morphology graded with HC-scoring was significantly increased in all experimental groups compared to the control ($p<0.001$) (Fig. 3-A, B). This increase was significantly greater in G3 compared to other groups ($p<0.001$) (Fig. 3-A, B). Moreover, there was also a significant increase in the number of degenerated both primary and secondary follicles in G3 compared to other groups ($p<0.05$) (Fig. 3-E, F). Since the morphology of primordial follicles was more preserved than other follicles in all groups, primordial follicles were not included in the follicle counting. Multiple comparisons and descriptive data for statistical analysis of HC-scoring and follicle counting are given in Fig. 3.

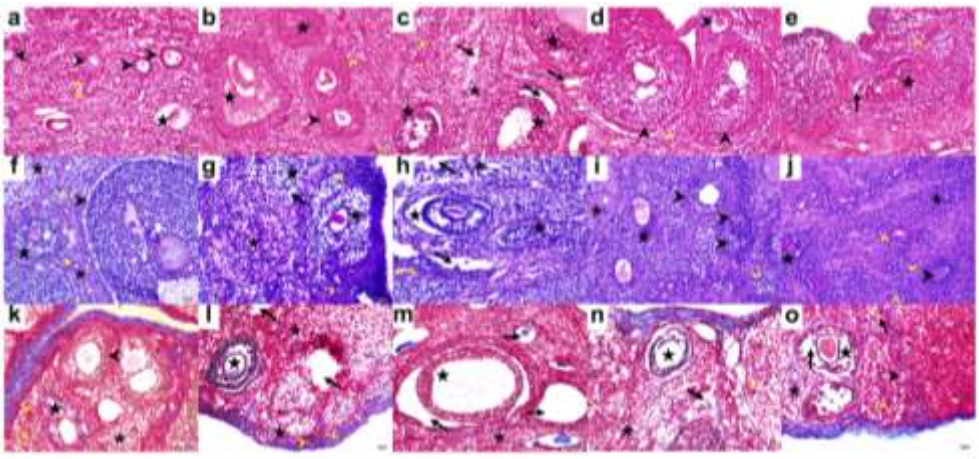

Fig. 2: Representative sections of HC stainings. Experimental groups (G1-G5) were arranged in columns, respectively. HC stainings of HE, PAS, and MT are given in rows, respectively. Regular histomorphology in G1 (a, f, k). Severe histomorphological damage with marked degeneration of primary and secondary follicles in G2 (b, g, l) and G3 (c, h, m). Tissue damage in G2 (b, g, l) is less than in G3 (c, h, m) and more pronounced than in G5 (e, j, o). G4 (d, i, n) with the least damage among all experimental groups. Scale bar = 20µm. Total magnification: 400x. *Arrowhead: healthy follicle; star: degenerated follicle; yellow arrowhead: primordial follicle; asterisk: stromal cells; black arrow: vacuolization or dissociation.*

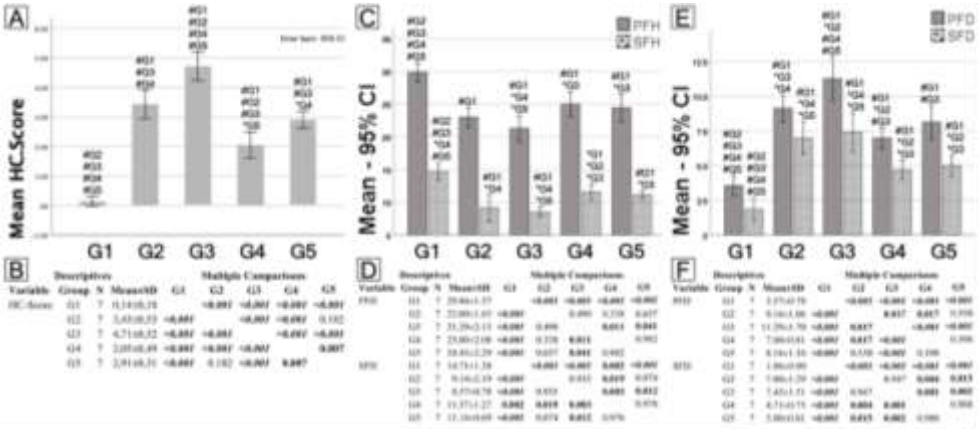

Fig. 3: Statistical results of HC-scoring and follicle counting. (**A-C-E**) Graphs of multiple comparisons of HC-score, healthy follicle counts, and degenerated follicle counts, respectively. (**B-D-F**) Descriptive data of A, C, and E, respectively. The results are given as the mean value (mean±SD). G1-5 refers to the study groups. Significance levels given as *<0.05 and **#**<0.001 in graphs reflect the significant results given in bold and bold/italics in descriptive data, respectively. *PFH, healthy primary follicle; PFD, degenerated primary follicle; SFH, healthy secondary follicle; SFD, degenerated secondary follicle.*

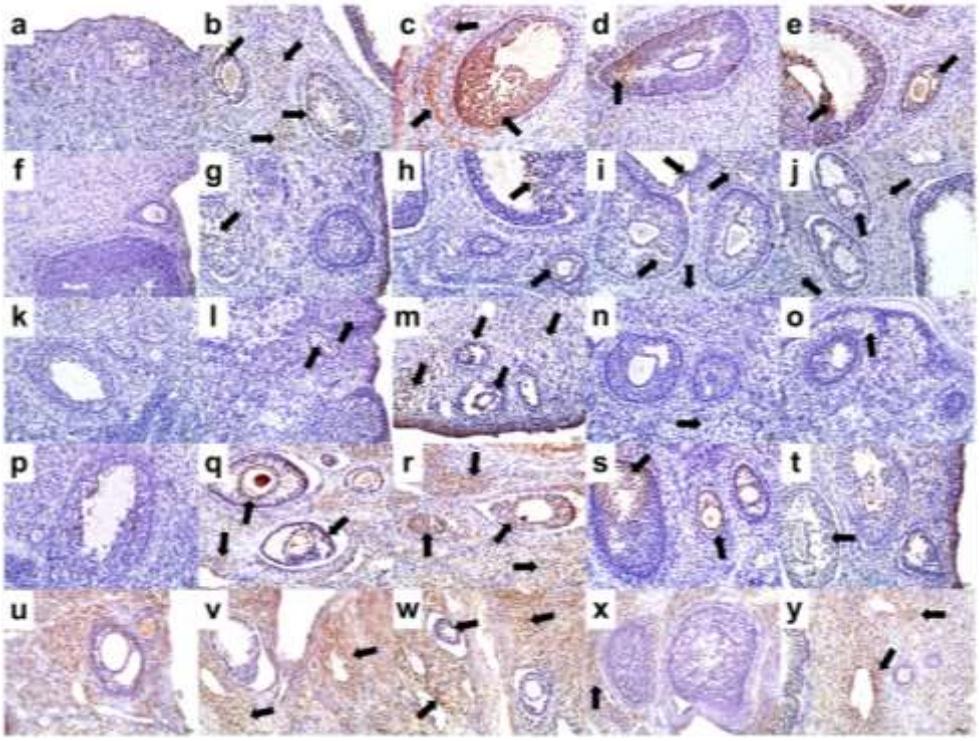

Fig. 4: Representative sections of IHC stainings. Experimental groups (G1-G5) are arranged in columns, respectively. Bax (a-e), Bcl-2 (f-j), C3 (k-o), Cx-43 (p-t) IHC staining, and TUNEL analysis (u-y) are given in rows, respectively. (**a-e**) Significant Bax immunoreactivity in G3. Partial reactivity in G4. (**f-j**) Weak Bcl-2 immunopositivity in G3. (**k-o**) Prominent C3 immunolabeling in G3 and G2, respectively. Weak positivity in G4. No reactivity in the primordial follicles of G4 and G5. (**p-t**) Prominent Cx-43 immunolabeling in G3 and G2, respectively. Weak positivity in G4. (**u-y**) Significant immunolabeling of TUNEL analysis at G3 and G2, respectively. Weak positivity in G4. Immunopositivity is indicated with the black arrow. Scale bar = 20µm. Total magnification: 400x.

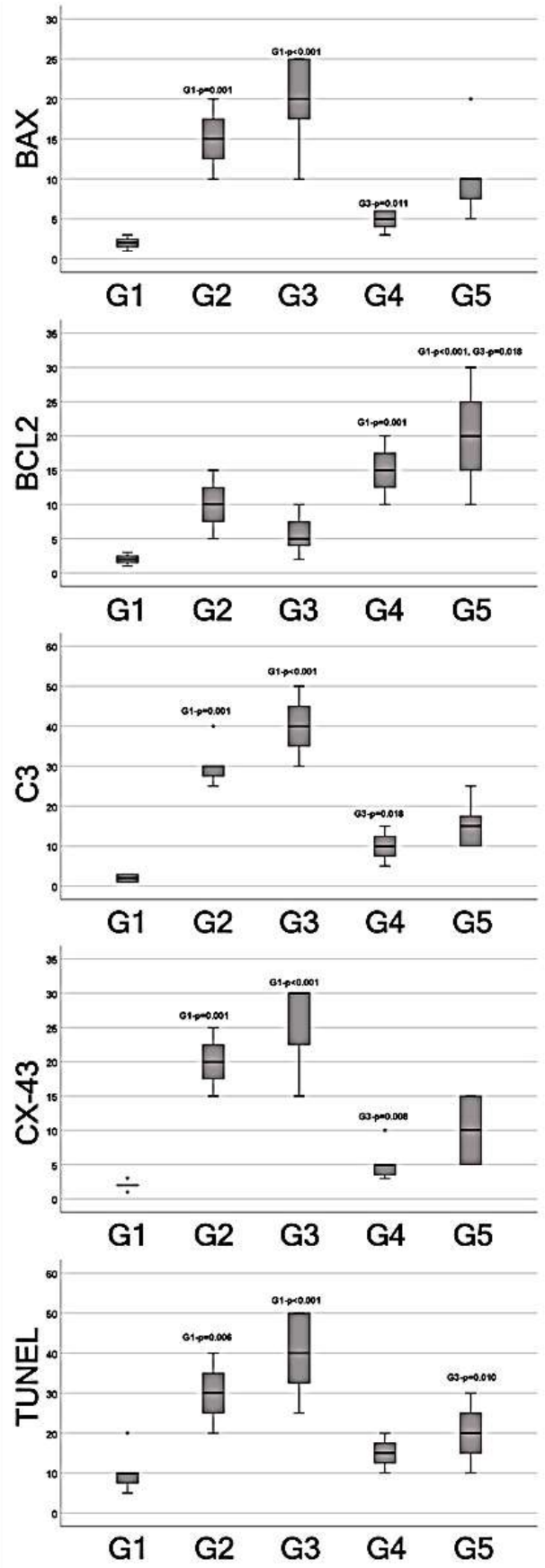

Fig. 5: Statistical results of IHC-scoring. Significant results (p<0.05) are given in bold. Dark line: median, bar: 25-75% of results, whiskers: min-max values.

Results of IHC assessment and TUNEL assay: Tissue sections showed a significant Bax immunoreactivity in G3 (Fig. 4c) and partial reactivity in G4 (Fig. 4d). Weak Bcl-2 immunopositivity is recorded in G3 (Fig. 4h). Prominent C3 immunolabeling is recorded in G3 (Fig. 4m) and G2 (Fig. 4l) respectively. Weak immunopositivity of C3 is noted in G4 (Fig. 4n) with no reactivity in the primordial follicles of G4 (Fig. 4n) and G5 (Fig. 4o). Prominent Cx-43 immunolabeling is observed in G3 (Fig. 4r) and G2 (Fig. 4q), respectively, and weak positivity in G4 (Fig. 4s). Significant immunolabeling of TUNEL analysis is noted in G3 (Fig. 4w) and G2 (Fig. 4v), respectively, with weak positivity in G4 (Fig. 4x). Representative sections of IHC stainings are given in Fig. 4.

Results of IHC and TUNEL assay scores: IHC scores of Bax, C3, Cx-43, and TUNEL assay were significantly higher in G2 (Bax, C3, and Cx-43, p<0.001; TUNEL, p=0.006) and in G3 (Bax, C3, Cx-43 and TUNEL, p<0.001) than other groups. The immunolabeling of Bcl-2 showed strong positivity in G4 and G5 compared to other groups (p<0.05). Multiple comparisons of IHC scores are given in Fig. 5.

DISCUSSION

OTCP is a unique technique to preserve fertility, but it is still not possible to prevent tissue degeneration (Marin *et al.*, 2020). To overcome cryoinjury and CPA toxicity, combinations of EG, DMSO, sucrose, and glycerol at different concentrations are being evaluated in animal studies (Gupta *et al.*, 2022). FBS is frequently used in experimental studies, but cannot be used in medical applications. Based on the assumption that PRP may have beneficial effects on OTCP due to platelet-derived cytokines that can improve the ovarian microenvironment, we preferred to use PRP instead of FBS. We expected PRP to reduce cryodamage with its antioxidant property.

Among the researchers working on cryoinjury prevention, there are those who report that primordial follicles representing the ovarian reserve tolerate cryoinjury better than developing follicles and are better preserved after ovarian tissue vitrification (Dupont *et al.*, 2022), and there are also those who claim the opposite (Ali Hassan *et al.*, 2023). Based on our results, we argue that EG, DMSO, and sucrose damage are less pronounced in primordial follicles and that PRP in the vitrification solution does not cause significant adverse effects in primordial follicles. Indeed, previous studies have associated less damage to primordial follicles with their lower cytoplasmic content and cellular features (Widad *et al.*, 2020; Gupta *et al.*, 2022). Since follicles other than primordial follicles were more damaged in our study, we hypothesize that this characteristic of primordial follicles is not valid for primary and secondary follicles. Indeed, more pronounced damage to primary and secondary follicles has been reported in previous studies (Kawai and Shimada, 2020; Sugishita *et al.*, 2021).

In our study, degeneration occurred more in primary and secondary follicles, and they exhibited cellular separations and irregularities in cell boundaries. The degenerated follicles were highest in G3, followed by G2, G5, and G4, respectively. Based on the previous reports, we hypothesize that the excess of degenerated follicles in G3 and G2 may have resulted from the vitrification process

(depending on the vitrification itself) (Fujiwara *et al.*, 2010), or from $CaCl_2$ used for the activation of PRP in the vitrification solution, or from the increase in mitochondrial and intracytoplasmic calcium caused by the CPAs used in the vitrification process (independent of the storage time in liquid nitrogen) (Cao *et al.*, 2022). Indeed, even though EG and DMSO are the most preferred CPAs and are widely used in vitrification procedures, both have been reported to increase both mitochondrial and intracytoplasmic calcium levels, causing zona pellucida hardening and ultimately fertilization failure in oocytes (Wang *et al.*, 2017; Cao *et al.*, 2022). Furthermore, the cryopreserved embryos and oocytes exhibited lower mitochondrial membrane potential (ΔΨm) and ATP content, which are markers for mitochondrial function (Len *et al.*, 2019).

We hypothesized that the increase in Cx-43 expression in G3 and G2 was due to the loss of lateral connections and the opening of hemichannels (unopposed hemichannels) (Van Campenhout *et al.*, 2021). We assumed that the pathological conditions in our study were oxidative and metabolic stress, which may have arisen from vitrification and possibly due to excess calcium in the vitrification solution. Recent cryopreservation studies have shown that abnormal opening of normally closed hemichannels due to vitrification and increased intracellular Ca2+ leads to an uncontrolled flow of metabolites and ions resulting in follicular cell death (Kordowitzki *et al.*, 2021). This has been demonstrated with TUNEL staining (Szymańska *et al.*, 2019).

Supporting this interpretation, TUNEL analysis results of our study coincided with our findings from Cx-43 IHC. Vitrification has also been suggested to significantly increase TUNEL immunopositivity in oocytes in association with low mitochondrial membrane potential (ΔΨm) (Len *et al.*, 2019). Granulosa cells showed more TUNEL-positive staining patterns in G3 and G2, suggesting they are more sensitive to cryopreservation due to the cholesterol molecule being more present in steroid-producing cells. A plausible explanation is that newly emerging pores in the membrane increased calcium influx into the cell, resulting in increased cellular damage. Recent studies recommend calcium-free solutions as a component of the vitrification solution (Marques *et al.*, 2018; Gualtieri *et al.*, 2021). Additionally, calcium chelators (Bonte *et al.*, 2020; Wang *et al.*, 2017) and purinergic receptor modulators (Fonseca *et al.*, 2020) have been reported to reduce cellular cryodamage.

Our study found that Bax was abundant in G3 and G2, predominantly in granulosa cells and oocytes, while Bcl-2 was fewer. Vitrification causes damage to the inner membrane of mitochondria and vesicular organelles, and the presence of Ca2+ in the vitrification solution may further increase this damage. Because as cell membranes are damaged, extracellular calcium penetrates more into the cell and activates apoptotic and inflammatory pathways, making antiapoptotic pathways ineffective. Similar results have been reported in vitrified bovine oocytes with a decrease in Bcl-2 mRNA expression and ΔΨm levels, and also, an increase in the levels of mCa^{2+}, Bax mRNA, C3 protein, DNA fragmentation, and ROS (Cao *et al.*, 2022).

C3 immunoexpression was most pronounced in G3 and G2, where the apoptotic markers were most and Bcl2 was least evident. In our study, Bcl-2 expression was higher in G4 and G5, and lower in G3 and G2. The Bcl-2 family may mediate suppression of Bax/Bak activity followed by inhibition of mitochondrial outer membrane permeability (MOMP) formation, leading to inhibition of cytochrome c release and effector caspases and thus inhibition of apoptosis (Warren *et al.*, 2019). We assume that the high Bcl-2 expression in G4 and G5 is due to the antiapoptotic effect that develops against cellular damage caused by vitrification-induced apoptosis. Contrary to expectations, the reason for the lower Bcl-2 expression seen in G3 and G2 is the excessive apoptotic effect due to cell damage caused by Ca^{2+} and increased excessive Bax expression. However, publications reporting both increased and decreased Bcl2 are evidence that Bcl-2 levels in vitrified ovarian tissues are controversial. A noteworthy review considered the results of several studies in a context with particular emphasis on the activation of apoptotic pathways in cryopreservation (Bahroudi *et al.*, 2022). An increase in the Bax expression and the percentage of Bax/Bcl-2 in the ovaries was associated with vitrification. In addition, the inhibition of the activation of C3 prevents the C3-mediated activation of enzymes that degrade the cell genome. Since some studies calculating the Bax/Bcl-2 ratio have discovered that high ratios indicate the tendency to apoptosis, the researchers emphasize that this ratio can be used as a marker of apoptosis and help predict the fate of the cell (Popgeorgiev *et al.*, 2020).

Conclusions: Vitrification has the potential to damage cell membranes and organelles and cause DNA fragmentation. However, we concluded that vitrification did not cause considerable damage to primordial follicles. We hypothesized that the PRP-added vitrification solution could improve cryopreservation outcomes in terms of tissue morphology. However, cryopreservation with PRP-supplemented vitrification solution (G3) significantly increased the degeneration severity ($p<0.05$). PRP used to reduce damage may have caused further cellular damage due to excessive $CaCl_2$ content, but further research is needed to confirm this.

Authorship confirmation/contribution statement: TÇ: Designed the experiment. TÇ, AG, CŞ, CT and KDK: Conducted research and collected the data. TÇ, AG, CŞ, CT, KDK and GY: Analyzed the data and finalized the write up of this manuscript

Conflicts of Interest: The authors declare that there is no conflict of interest.

Funding Statement: This study is supported by Ege University Scientific Research Projects Coordination Unit (Project Number: TKB-2019-20518).

REFERENCES

Ali Hassan H, Banchi P, Chayaa R, *et al*., 2023. Feline ovarian tissue vitrification: The effect of fragment size and base medium on follicular viability and morphology. Theriogenology 198:12–8.

Bahroudi Z, Zarnaghi MR, Izadpanah M, *et al*., 2022. Review of ovarian tissue cryopreservation techniques for fertility preservation. J Gynecol Obstet Hum Reprod 51:102290.

Bonte D, Thys V, De Sutter P, *et al.,* 2020. Vitrification negatively affects the Ca2+-releasing and activation potential of mouse oocytes, but vitrified oocytes are potentially useful for diagnostic purposes. Reprod Biomed Online 40:13–25.

Van Campenhout R, Gomes AR, De Groof TWM, *et al*., 2021. Mechanisms underlying connexin hemichannel activation in disease. Int J Mol Sci 22:3503.

Cao B, Qin J, Pan B, *et al*., 2022. Oxidative stress and oocyte cryopreservation: recent advances in mitigation strategies involving antioxidants. Cells 11:3573.

Chen NF, Sung CS, Wen ZH, *et al*., 2018. Therapeutic effect of platelet-rich plasma in rat spinal cord injuries. Front Neurosci 12:252.

Dupont Á, Sanguinet E, Ferreira M, *et al*., 2022. Morphological study on the effects of sample size on ovarian tissue vitrification. J Bras Reprod Assist 26:374–78.

Fonseca E, Mesquita P, Marques CC, *et al*., 2020. Modulation of P2Y2 receptors in bovine cumulus oocyte complexes: effects on intracellular calcium, zona hardening and developmental competence. Purinergic Signal 16:85–96.

Fujiwara K, Sano D, Seita Y, *et al*., 2010. Ethylene glycol-supplemented calcium-free media improve zona penetration of vitrified rat oocytes by sperm cells. Journal of Reproduction and Development 56:169–75.

Gandolfi F, Paffoni A, Papasso Brambilla E, *et al*., 2006. Efficiency of equilibrium cooling and vitrification procedures for the cryopreservation of ovarian tissue: comparative analysis between human and animal models. Fertil Steril 85 Suppl 1:1150–56.

Gualtieri R, Kalthur G, Barbato V, *et al*., 2021. Mitochondrial dysfunction and oxidative stress caused by cryopreservation in reproductive cells. Antioxidants (Basel) 10:337.

Gupta PSP, Kaushik K, Johnson P, *et al*., 2022. Effect of different vitrification protocols on post thaw viability and gene expression of ovine preantral follicles. Theriogenology 178:1–7.

He ZY, Wang HY, Zhou X, *et al*., 2018. Evaluation of vitrification protocol of mouse ovarian tissue by effect of DNA methyltransferase-1 and paternal imprinted growth factor receptor-binding protein 10 on signaling pathways. Cryobiology 80:89–95.

Kawai T and Shimada M, 2020. Pretreatment of ovaries with collagenase before vitrification keeps the ovarian reserve by maintaining cell-cell adhesion integrity in ovarian follicles. Sci Rep 10:6841.

Kinnear HM, Tomaszewski CE, Chang FL, *et al*., 2020. The ovarian stroma as a new frontier. Reproduction 160:25–39.

Kordowitzki P, Sokołowska G, Wasielak-Politowska M, *et al*., 2021. Pannexins and Connexins: Their relevance for oocyte developmental competence. Int J Mol Sci 22:5918.

Len JS, Koh WSD and Tan S-X, 2019. The roles of reactive oxygen species and antioxidants in cryopreservation. Biosci Rep 39.

Marin L, Bedoschi G, Kawahara T, *et al*., 2020. History, evolution and current state of ovarian tissue auto-transplantation with cryopreserved tissue: a successful translational research journey from 1999 to 2020. Reprod Sci 27:955–62.

Marques CC, Santos-Silva C, Rodrigues C, *et al*., 2018. Bovine oocyte membrane permeability and cryosurvival: Effects of different cryoprotectants and calcium in the vitrification media. Cryobiology 81:4–11.

Merhi Z, Seckin S and Mouanness M, 2022. Intraovarian PRP injection improved hot flashes in a woman with very low ovarian reserve. Reprod Sci 29:614–19.

Oktay K, 2022. Principles and practice of ovarian tissue cryopreservation and transplantation. Elsevier: US.

Popgeorgiev N, Sa JD, Jabbour L, *et al*., 2020. Ancient and conserved functional interplay between Bcl-2 family proteins in the mitochondrial pathway of apoptosis. Sci Adv 6:eabc4149.

Practice Committee of the American Society for Reproductive Medicine, 2019. Fertility preservation in patients undergoing gonadotoxic therapy or gonadectomy: a committee opinion. Fertil Steril 112:1022–33.

Schallmoser A, Einenkel R, Färber C, *et al*., 2022. The effect of high-throughput vitrification of human ovarian cortex tissue on follicular viability: a promising alternative to conventional slow freezing? Arch Gynecol Obstet 307:591–99.

Sugishita Y, Taylan E, Kawahara T, *et al*., 2021. Comparison of open and a novel closed vitrification system with slow freezing for human ovarian tissue cryopreservation. J Assist Reprod Genet 38:2723-33.

Szymańska KJ, Ortiz-Escribano N, Van den Abbeel E, *et al*., 2019. Connexin hemichannels and cell death as measures of bovine COC vitrification success. Reproduction 157:87–99.

Wang N, Hao HS, Li CY, *et al*., 2017. Calcium ion regulation by BAPTA-AM and ruthenium red improved the fertilisation capacity and developmental ability of vitrified bovine oocytes. Sci Rep 7:10652.

Warren CFA, Wong-Brown MW and Bowden NA, 2019. BCL-2 family isoforms in apoptosis and cancer. Cell Death Dis 10:177.

Widad S, Nurdiati DS, Ayuandari S, *et al*., 2020. Primordial follicle survival of goat ovarian tissue after vitrification and transplantation on chorioallanthoic membrane. Middle East Fertil Soc J 25:34.